Raman scattering study of stoichiometric Si and Ge type II clathrates

G. S. Nolas[a)]
Department of Physics, University of South Florida, Tampa, Florida 33620

C. A. Kendziora
Materials Science and Technology Division, Code 6330, Naval Research Laboratory, Washington, DC 20375

Jan Gryko
Department of Physical and Earth Sciences, Jacksonville State University, Jacksonville, Alabama 36265

Jianjun Dong
Department of Physics, Auburn University, Auburn, Alabama 36849

Charles W. Myles
Department of Physics and Astronomy, Arizona State University, Tempe, Arizona 85287

Abhijit Poddar and Otto F. Sankey
Department of Physics and Engineering Physics, Texas Tech University, Lubbock, Texas 79409

(Received 16 August 2002; accepted 27 September 2002)

Raman-scattering spectra of the type II clathrates $Cs_8Na_{16}Si_{136}$, $Cs_8Na_{16}Ge_{136}$, and Si_{136} were studied employing different laser wavelengths. Most of the Raman-active vibrational modes of these compounds were identified. Polarization measurements were used to identify the symmetric modes. The lowest frequency Raman-active optic ''rattle'' mode corresponding to the vibrations of the Cs atoms inside the hexakaidecahedra is identified for both the Si and the Ge clathrate compounds. We compare the experimental data directly with theoretical calculations. These materials continue to attract attention for potential superconducting, optoelectronic, and thermoelectric applications. © *2002 American Institute of Physics.* [DOI: 10.1063/1.1523146]

INTRODUCTION

Materials with the clathrate hydrate crystal structure belong to a class of zeolite-like compounds formed by group-IV elements. These materials continue to attract considerable interest due to their unique transport properties. It is believed that these materials can be developed for thermoelectric,[1–4] superconducting,[5–8] and electro-optic applications.[9,10] Among the novel properties these compounds possess is their low thermal conductivity due to the weak bonding of the guest atoms residing inside atomic ''cages'' formed by the host atoms. This results in localized vibrational modes which couple to the lattice modes, thus resonantly scattering the acoustic-mode, heat-carrying phonons.[1]

Of the two clathrate types, the type I clathrate hydrate crystal structure has been more fully investigated experimentally. Thus far both transport and optical properties of type I clathrates have been published. The low thermal conductivity measured in compounds with the type I clathrate structure is due to the weak guest–host interactions whereby the localized guest vibrations interact strongly with the host acoustic modes. The evidence for this model includes thermal transport,[11–18] Raman scattering,[19] and acoustic measurements[20,21] as well as theoretical calculations.[22,23]

The type II clathrates have not been as well investigated. The vibrational modes of the type II ''empty'' clathrates Si_{136} (Refs. 24–27) and Ge_{136} (Ref. 27) have been theoretically investigated due to their potential application for superconductivity and thermoelectrics. Raman scattering spectra of Na_xSi_{136} have also been previously reported.[28] Recently structural properties have been reported for stoichiometric Si and Ge clathrates, i.e., with all the crystallographic sites within the polyhedra of the type II structure occupied.[29–31] The stoichiometric compounds $Cs_8Na_{16}Si_{136}$ and $Cs_8Na_{16}Ge_{136}$ possess metallic conduction, as indicated by transport[31] and nuclear magnetic resonance[32,33] measurements. In addition, temperature dependent single crystal x-ray diffraction measurements estimate the low lying vibrational modes of the Cs atoms inside these Si and Ge type II clathrates to be 53 and 42 cm^{-1}, respectively.[31]

In this article we present a Raman spectroscopic analysis of polycrystalline and single crystal $Cs_8Na_{16}Si_{136}$ and $Cs_8Na_{16}Ge_{136}$. The Raman spectrum of Si_{136}, a type II clathrate with no guest atoms inside the polyhedra formed by the Si framework atoms, is used for a reference to experimentally identify the alkali-metal ''rattle'' modes of $Cs_8Na_{16}Si_{136}$. We record polarized Stokes spectra at two different nonresonant laser wavelengths. We employ density functional, plane-wave pseudopotential calculations to calculate the vibrational modes of $Cs_8Na_{16}Si_{136}$ and $Cs_8Na_{16}Ge_{136}$, and compare these with our experimental results. In addition, we compare our measured vibrational modes in Si_{136} with the theoretical calculations of Ref. 26.

[a)]Author to whom correspondence should be addressed; electronic mail: gnolas@chumal.cas.usf.edu

TABLE I. Compositional and structural properties of the type II clathrate specimens prepared for Raman scattering measurements. The atomic percentages from electron-beam microprobe analysis, the experimental lattice parameter (a_0) in angstroms, the measured density (D_{meas}) in g/cm^3, and the theoretical density (D_{theory}) in g/cm^3.

Compound	elemental at. %	a_0	D_{meas}	D_{theory}
$Cs_8Na_{16}Si_{36}$	4.95Cs/10.77Na/84.28Si	14.7402	2.6	2.72
Si_{136}		14.6260	1.4	2.01
$Cs_8Na_{16}Ge_{136}$	5.06Cs/10.16Na/84.78Ge	15.4792	4.8	5.06

SAMPLE PREPARATION AND EXPERIMENTAL ARRANGEMENT

Single crystal and polycrystalline specimens were employed in this work. Small single crystals of $Cs_8Na_{16}Si_{136}$ and $Cs_8Na_{16}Ge_{136}$ were prepared by reacting the high purity elements for three weeks at 650 °C inside a tungsten crucible that was itself sealed inside a stainless steel canister. The canister contained a nitrogen atmosphere at ambient pressure and temperature. After maintaining a 650 °C temperature, the contents were cooled to room temperature at a rate of 0.2 °C/min. The resulting compounds consisted of small, shiny crystals that have a bluish metallic luster. Several of the smaller single crystals were isolated and investigated employing an Enraf-Nonius CAD-4 diffractometer. These data could be indexed to the type II clathrate structure (Fd-$3m$ space group). Si_{136} was prepared by a modified degassing procedure first described by Gryko *et al.*[10] Sodium silicide was degassed at 385 °C at $\sim 10^{-5}$ Torr for several days. The resulting mixture of Na_xSi_{136} ($x<4$) and Na_8Si_{46} was density separated using $CCl_4+CH_2Br_2$ solution to obtain Na_xSi_{136} samples free of Si_{46} phase. Na_xSi_{136} was then washed in concentrated hydrochloric acid, dried, and degassed again under high vacuum for several days. The process of washing with HCl and degassing was repeated several times with degassing temperature increasing from 395 to 430 °C. The final Si_{136} compound had a sodium content of less than 100 ppm. In order to create dense polycrystalline pellets for microscopic as well as Raman measurements the $Cs_8Na_{16}Si_{136}$ and $Cs_8Na_{16}Ge_{136}$ specimens were ground to fine powders and hot pressed inside graphite dies at 700 and 380 °C, respectively, and 2 kbar for 2 h in an argon atmosphere. This resulted in dense pellets with greater than 95% of theoretical density. The Si_{136} specimen was cold pressed at 15 kbar to approximately 70% of theoretical density.

The polycrystalline specimens were then cut with a wire saw and polished to a final mirror-like surface with 0.3 μm alumina paste. Small single crystals of $Cs_8Na_{16}Si_{136}$ and $Cs_8Na_{16}Ge_{136}$ were mounted in epoxy and similarly polished for Raman scattering measurements. Electron-beam microprobe analysis of the polished cross section of the stoichiometric type II clathrate specimens revealed the exact composition of our specimens. Table I summarizes these data for the specimens prepared for this work. Powder x-ray diffraction was also employed on the polycrystalline specimens with no impurity lines, or spectra from amorphous Si or Ge, in the case of the two alkali-metal filled specimens. The Si_{136} specimen showed trace amounts of diamond structure Si.

The 457.9 and 514.5 nm excitation of an Ar-ion laser, 647.1 nm excitation of a Kr-ion laser, and 700 nm excitation of a Ti-sapphire laser were used in the Raman-scattering measurements. The incident beam was backscattered off the sample at a 45° angle to avoid the direct reflection impinging on the collection lens. The collected light was analyzed with a Dilor 500 mm triple-grating spectrometer and counted with a liquid-nitrogen-cooled charge coupled device (CCD) array. To prevent surface damage, the power incident onto the sample was limited to less than 75 mW. Typical collection times were 15–20 min and several scans were averaged to increase the signal-to-noise ratio and remove anomalous spikes. The spectral resolution was 3 cm^{-1} for the blue and green excitations, and 2 cm^{-1} for red excitation. Low temperature (10 K) measurements were also performed, however, with lower incident power in flowing He vapor to minimize the effects of laser heating. The 10 K spectra were similar to those obtained at room temperature, with no new phonons and minimal frequency shifts between the two temperatures. We thus employ the room temperature data to fit the spectra and tabulate the Raman lines in this report.

COMPUTATIONAL APPROACH

We employ density functional theory in the local density approximation (LDA) to determine the theoretical vibrational mode frequencies. For large unit cells such as the type II clathrates, a computationally efficient method must be applied. For this purpose we used the VASP code.[34–36] This methodology utilizes a pseudopotential approximation so that only the valence electrons, and not the atomic core states, are considered. The basis states are plane waves; these are advantageous for framework materials since they describe the regions inside cages on an equal footing with regions near the atoms.

The structural parameters used for the calculation of the vibrational modes were obtained from optimizing the structure to its lowest energy. The resulting theoretical cubic lattice constants of the Fd-$3m$ lattices are 14.55, 14.56, and 15.39 Å for Si_{136}, $Cs_8Na_{16}Si_{136}$, and $Cs_8Na_{16}Ge_{136}$, respectively. These values are in good agreement with our x-ray values of 14.63, 14.74, and 15.48 Å, respectively, as shown in Table I. The percentage difference between the theoretical and experimental values are 0.55%, 1.36%, and 0.6%, respectively. It is interesting to note that the largest difference is for the loaded Si, for which theory does not reproduce the expansion on loading as seen in experiment. Loading Si_{136} to $Cs_8Na_{16}Si_{136}$ changes the material from a semiconductor to a metal. We speculate that the local density approximation for exchange, which energetically favors high density (particularly inside the cages), tends to compensate for the expansion of the cages encouraged by the additional occupation of antibonding states within the conduction band that loading produces.

The vibrational modes were determined from the forces produced by finite displacements of atoms. Point group symmetry is used to reduce the problem from $3N$ variables (N = number of atoms in the unit cell) to a minimum number of independent displacements. The use of symmetry yields the

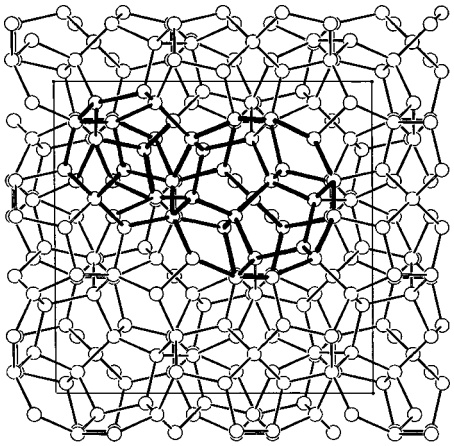

FIG. 1. The type II clathrate hydrate crystal structure. Outlined are the two different polyhedra that form the unit cell. Only the group-IV atoms are shown. Guests (such as Cs and Na) may reside within the cages.

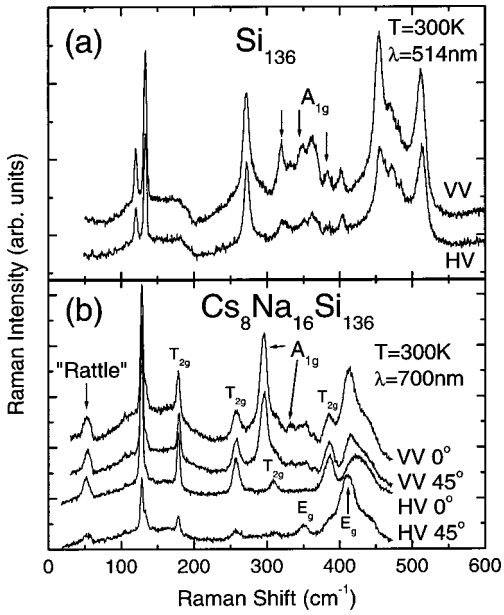

FIG. 2. The room temperature ($T=300$ K) parallel (VV) and perpendicular (HV) polarized Stokes Raman scattering spectra of (a) polycrystalline Si_{136} using 514.5 nm excitation and (b) single crystal $Cs_8Na_{16}Si_{136}$ using 700 nm excitation. For comparison purposes the curves are offset by an additive factor in intensity. The difference in intensity between parallel and perpendicular polarization identifies the A_{1g} modes. In (a) the mode at 511 cm^{-1} is likely from diamond structured Si present in our Si_{136} specimen in trace amounts. In (b) an arrow points to the vibrational "rattle" mode at 57 cm^{-1} associated with the Cs atom within the hexakaidecahedra. Spectra taken for two different orientations at the same spot on the $Cs_8Na_{16}Si_{136}$ crystal reveal two distinct symmetries (E_g and T_{2g}) for several of the framework modes. Exact assignments were done with the help of our theoretical modes assignments.

$\mathbf{q}=(000)$ dynamical matrix from just six independent atomic displacements. The procedure is to displace a single atom from equilibrium along a Cartesian direction by a distance small U_0 and determine the forces on all atoms. Dividing each of the $3N$ forces by the displacement yields a full row of the dynamical matrix. Repeating this for all independent displacements, and using symmetry, produces the entire dynamical matrix from which eigenvalues (frequencies) are determined. More details of phonon calculations can be found in Refs. 26 and 27.

RESULTS AND DISCUSSION

The type II clathrate hydrate crystal structure is face-centered cubic with the $Fd\text{-}3m$ space group. The general formula is $Cs_8Na_{16}Z_{136}$ where Z=Si or Ge. There are three distinct crystallographic sites that form the Z framework, the $8a$, $32e$, and $96g$ sites. The framework can be thought of as being constructed by connecting Z_{20} and Z_{28} polyhedra together with shared faces. Figure 1 is a schematic of the type II clathrate crystal lattice structure. There are 120 (3×40) Γ-point ($\mathbf{q}=0$) phonon modes, not counting degeneracies, from the 40 atoms per primitive cell of the framework and guests. From these the first order Raman-active modes of the framework are $3A_{1g}+4E_g+8T_{2g}$. The Cs atoms reside inside the eight hexakaidecahedra, at the $8b$ crystallographic sites, and the Na atoms reside inside the 16 dodecahedra, at the $16c$ sites, per cubic unit cell. The Cs atoms contribute a Raman-active T_{2g} mode while the Na atoms do not contribute Raman-active optic modes. In total therefore there are 16 Raman-active modes in stoichiometric type II clathrates and 15 modes in Si_{136}.

Figure 2 shows room temperature ($T=300$ K) Stokes Raman spectra for the (a) Si_{136} and (b) $Cs_8Na_{16}Si_{136}$ specimens in parallel (VV) and perpendicular (HV) polarizations of the incident and collected light. The spectra have been offset by an additive factor on the intensity axis for convenient visualization. The spectral resolution was 3 cm^{-1} for $\lambda=514$ nm and 2 cm^{-1} for $\lambda=700$ nm, allowing us to observe sharp features with linewidths (full width at half-maximum, FWHM) that are in general narrower than those previously measured in Na_xSi_{136}. [28] We have used the anti-Stokes spectra and spectra from four different laser wavelengths (not shown) in order to separate the Raman signal in these clathrate compounds from artifacts.

The results of our fits to the Raman data as well as our eigenmode calculations are summarized in Table II. We assign each experimentally observed mode to a predicted one based on both the frequency and symmetry. Several of the expected modes may have Raman intensity below our detection limit or they may simply not be resolved within a broad peak. As a result, we identify only 13 Raman phonons for $Cs_8Na_{16}Si_{136}$ and 14 for Si_{136}. For the silicon-based materials (the first four columns of Table II), the assignments are grouped by row, with only the two highest frequency vibrations falling in reverse order for the ternary compound when compared to the "empty" Si_{136}. To determine mode symmetry experimentally, we utilized the polarization selection rules. Despite the fact that our Si_{136} measurements were performed on polycrystalline specimens, we can still distinguish the fully symmetric A_{1g} modes by the ratio of their intensity in parallel (VV) to crossed (HV) polarization. This is only true because the scattered light averages over a large number of scattering centers due to the fact that our grain sizes are smaller than the incident beam focus. Contrary to previous measurements on Na_xSi_{136}, [28] we observe significant polarization dependence in the A_{1g} modes.

TABLE II. The theoretically calculated Raman-active modes, compared with experimental peak positions and FWHM, both in cm^{-1}, for $Cs_8Na_{16}Si_{136}$, Si_{136} and $Cs_8Na_{16}Ge_{136}$ are tabulated. Similar mode assignments are on the same row for the case of the Si-clathrates, requiring that the two highest frequency modes for Si_{136} be listed in reverse order of frequency. The first row displays the vibrational ''rattle'' modes of Cs. The theoretical data for Si_{136} are from Ref. 19. Experimental peaks listed with a caret exhibited significantly greater intensity in VV than HV polarization and are therefore assigned to modes of A_{1g} symmetry. The latter ''s'' indicates a wide FWHM that is not fully resolved from neighboring modes (e.g., a shoulder next to a strong mode).

$Cs_8Na_{16}Si_{136}$ theory	$Cs_8Na_{16}Si_{136}$ experiment	Si_{136} theory	Si_{136} experiment	$Cs_8Na_{16}Ge_{136}$ theory	$Cs_8Na_{16}Ge_{136}$ experiment
64 (T_{2g})	57 (10)			21 (T_{2g})	18 (6)
118 (T_{2g})	126 (s)	121 (T_{2g})	120 (3)	55 (E_g)	42 (7)
131 (E_g)	135 (10)	130 (E_g)	133 (5)	57 (T_{2g})	62 (8)
165 (T_{2g})	173 (s)	176 (T_{2g})	165 (6)		67 (4)
258 (T_{2g})	262 (16)	267 (T_{2g})	272 (12)	80 (T_{2g})	85 (26)
284 (A_{1g})	299^ (25)	316 (A_{1g})	320^ (7)	126 (T_{2g})	143 (13)
306 (T_{2g})	320 (15)	325 (T_{2g})	333 (3)	158 (T_{2g})	
			347^ (18)	159 (A_{1g})	164^ (22)
349 (E_g)	355 (28)	360 (E_g)	362 (8)	186 (E_g)	180 (18)
374 (A_{1g})	335^ (20)	397 (A_{1g})	383^ (3)	212 (T_{2g})	
387 (T_{2g})	390 (19)	406 (T_{2g})	404 (9)	213 (A_{1g})	
411 (A_{1g})		458 (A_{1g})		231 (T_{2g})	222 (9)
414 (E_g)	416 (22)	463 (E_g)	454 (17)	231 (E_g)	
416 (T_{2g})		466 (T_{2g})	467 (15)	233 (A_{1g})	
426 (T_{2g})		473 (T_{2g})	471 (9)	242 (T_{2g})	257 (13)
443 (T_{2g})	444 (32)	487 (T_{2g})	490 (12)	248 (T_{2g})	265 (s)
449 (E_g)	478 (s)	483 (E_g)		249 (E_g)	

Although we did not align our small single crystal $Cs_8Na_{16}Si_{136}$ specimens along specific crystallographic axes for symmetry-specific polarization measurements, distinguishing *between* the T_{2g} and E_g modes for several of the experimental modes was accomplished by rotating the specimen about an axis normal to its surface. Exact mode assignments for the T_{2g} and E_g modes shown in Fig. 2(b) were done with the help of the calculations. We note that the agreement between experiment and theory (Table II) is quite good. This is very encouraging given the complexity and large number of atoms per unit cell in the type II clathrates. In an earlier comparison with experiment in Ref. 28 to tight-binding theory, the agreement between theory and experiment was not found to be as satisfactory. The present theoretical method uses a complete basis set (plane waves), and is able to describe with equal accuracy the metal atoms and the semiconductor atoms. These improvements produce a compelling theory/experiment comparison.

The framework Raman modes of $Cs_8Na_{16}Si_{136}$ resemble those of Si_{136}. Experimentally, the higher frequency Si framework modes (above 300 cm^{-1}) of $Cs_8Na_{16}Si_{136}$ are shifted towards lower frequency as compared to those of Si_{136}, as predicted by our calculations. The framework modes below 300 cm^{-1} remain relatively unperturbed, indicating that the metal–framework interaction has a stronger effect on the higher frequency optic modes. Physically, the higher frequency modes tend to originate from bond stretches between a pair of Si framework atoms. The ''guest-free'' Si_{136} material is a semiconductor, while $Cs_8Na_{16}Si_{136}$ is a metal. In a rigid band picture (which, while of limited validity, may be instructive in this case), the additional electrons from Cs and Na are donated to the framework conduction bands. These bands are primarily antibonding states; occupying these reduces the Si–Si bond order to a value less than that of a single bond. This diminishes the restoring stretch force and reduces the frequency.

Figure 3 shows room temperature Stokes Raman spectra for $Cs_8Na_{16}Ge_{136}$ using the 514.5 nm Ar^+ laser line for parallel (VV) and perpendicular (HV) polarizations. The peak positions and FWHM of the experimentally determined Raman-active modes as well as our theoretical assignments are included in Table II for comparison with each other as well as with the silicon clathrates. Although the polarization selection was less obvious in this material than for either of the Si type II (probably due to peak overlap and low Raman

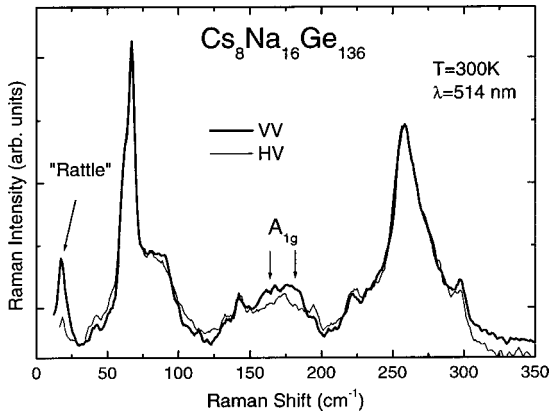

FIG. 3. The Stokes Raman scattering spectra of polycrystalline $Cs_8Na_{16}Ge_{136}$ in parallel (VV) and perpendicular (HV) polarization at room temperature ($T=300$ K) with 514.5 nm excitation. An arrow points to the vibrational ''rattle'' mode at 18 cm^{-1} associated with the Cs atom within hexakaidecahedra. The small peak at 298 cm^{-1} is possibly due to diamond structured Ge.

intensity for the A_{1g} modes), the small peaks at 164 and 180 cm^{-1} may have A_{1g} symmetry. The relationship between the experimentally identified framework modes of $Cs_8Na_{16}Ge_{136}$ and the theoretically calculated modes of Ge_{136} (Ref. 27) is evident.

The Raman spectra of $Cs_8Na_{16}Si_{136}$ and $Cs_8Na_{16}Ge_{136}$ are generally similar to each other. The optical modes of the Ge-clathrate shifted to lower frequencies as compared to that of the Si-clathrate because of the difference in the atomic weight and the bond length of Si compared with those of Ge. An estimate of the effect of the mass difference on bond strength indicates that this, indeed, has a large affect since $\sqrt{M_{Ge}}/\sqrt{M_{Si}}=1.6$. This value is comparable to the experimentally observed shift upward in the framework mode frequencies by a factor of ~1.8 times higher for $Cs_8Na_{16}Si_{136}$ in comparison with those of $Cs_8Na_{16}Ge_{136}$ [see Figs. 2(b) and 3 and Table II]. We note that this is also very similar to the ratio of the Raman frequency of diamond-Si to that of diamond-Ge.[37] In both stoichiometric clathrates the lowest Raman-active vibrational mode is assigned to an optical vibrational mode of the ''guest'' Cs atom inside the hexakaidecahedral ''cage.'' This mode is indicated with an arrow in Figs. 2 and 3. These Cs ''rattle'' modes are in reasonably good agreement with estimates obtained from temperature dependent atomic displacement parameters from single crystal x-ray measurements.[31] Density functional calculations indicate the acoustic phonons to be below 60 cm^{-1} for Ge_{136} (Ref. 27) and below 100 cm^{-1} for Si_{136}.[26] This places the Cs ''rattle'' modes well within the acoustic phonons in each compound. These optic modes may therefore resonantly scatter the acoustic phonons, as in the case of the type I clathrates, resulting in very low lattice thermal conductivities. An investigation of the thermal properties of semiconductor variants of alkali-metal filled type II clathrates would therefore be of interest for understanding novel phonon-scattering mechanisms.

CONCLUSION

Of the group-theory predicted 16 Raman-active optic modes of the stoichiometric type II clathrate $Cs_8Na_{16}Si_{136}$ we have experimentally identified and assigned 13. We have also identified and assigned 10 of the 16 modes of $Cs_8Na_{16}Ge_{136}$ and 13 of the 15 modes of Si_{136}. The vibrational modes associated with the framework atoms range from 120 to 490 cm^{-1} for $Cs_8Na_{16}Si_{136}$ and 42 to 265 cm^{-1} for $Cs_8Na_{16}Ge_{136}$. The agreement between theory and experiment is very strong and lends confidence to our mode assignments. The localized ''rattle'' modes of Cs inside the hexakaidecahedra were also identified at 57 and 18 cm^{-1} for $Cs_8Na_{16}Si_{136}$ and $Cs_8Na_{16}Ge_{136}$, respectively. These modes are in the range of the acoustic phonons in this crystal structure. The localized phonon-scattering centers created by the dynamic disorder of the Cs atoms encapsulated in their atomic ''cages'' may resonantly scatter with the framework acoustic phonons and result in low thermal conductivities in semiconducting variants.

ACKNOWLEDGMENTS

The authors thank T. J. R. Weakley for single crystal x-ray diffraction measurements. G.S.N. acknowledges support from the University of South Florida. This work was initiated through support from the U.S. Army Research Laboratory under Contract No. DAAD17-99-C-0006 and Marlow Industries, Inc. The National Science Foundation supported the work at Arizona State University (NSF DMR-99-86706). The experiments performed at NRL were supported by ONR.

[1] G. S. Nolas, G. A. Slack, and S. B. Schujman, in *Semiconductors and Semimetals*, edited by T. M. Tritt (Academic, San Diego, 2000), Vol. 69, p. 255, and references therein.
[2] G. S. Nolas, J. W. Sharp, and H. J. Goldsmid, *Thermoelectrics: Basic Principles and New Materials Developments* (Springer-Verlag, Heidelberg, 2001).
[3] N. P. Blake, S. Latturner, J. D. Bryan, G. D. Stucky, and H. Metiu, J. Chem. Phys. **115**, 8080 (2001).
[4] V. L. Kuznetsov, L. A. Kuznetsova, A. E. Kaliazin, and D. M. Rowe, J. Appl. Phys. **87**, 7871 (2000).
[5] J. D. Bryan, V. I. Srdanov, G. D. Stucky, and D. Schmidt, Phys. Rev. B **60**, 3064 (1999).
[6] S. Yamanaka, E. Enishi, H. Fukluoka, and M. Yasukawa, Inorg. Chem. **39**, 56 (2000).
[7] T. Yokoya, A. Fukushima, T. Kiss, K. Kobayashi, S. Shin, K. Moriguchi, A. Shintani, H. Fukuoka, and S. Yamanaka, Phys. Rev. B **64**, 172504 (2001).
[8] F. M. Grosche, H. Q. Yuan, W. Carrillo-Cabrera, S. Paschen, C. Langhammer, F. Kromer, G. Sparn, M. Baenitz, Yu. Grin, and F. Steglich, Phys. Rev. Lett. **87**, 247003 (2001).
[9] G. B. Adams, M. O'Keeffe, A. A. Demkov, O. F. Sankey, and Y. Huang, Phys. Rev. B **49**, 8048 (1994).
[10] J. Gryko, P. F. McMillan, R. F. Marzke, G. K. Ramachandran, D. Patton, S. K. Deb, and O. F. Sankey, Phys. Rev. B **62**, R7707 (2000).
[11] J. S. Tse and M. A. White, J. Phys. Chem. **92**, 5006 (1998).
[12] G. S. Nolas, J. L. Cohn, G. A. Slack, and S. B. Schujman, Appl. Phys. Lett. **73**, 178 (1998).
[13] J. L. Cohn, G. S. Nolas, V. Fessatidis, T. H. Metcalf, and G. A. Slack, Phys. Rev. Lett. **92**, 779 (1999).
[14] G. S. Nolas, T. J. R. Weakley, J. L. Cohn, and R. Sharma, Phys. Rev. B **61**, 3845 (2000).
[15] B. C. Chakoumakos, B. C. Sales, D. G. Mandrus, and G. S. Nolas, J. Alloys Compd. **296**, 80 (1999).
[16] G. S. Nolas, B. C. Chakoumakos, B. Mahieu, G. J. Long, and T. J. R. Weakley, Chem. Mater. **12**, 1947 (2000).
[17] B. C. Sales, B. C. Chakoumakos, R. Jin, J. R. Thompson, and D. Mandrus, Phys. Rev. B **63**, 245113 (2001).
[18] S. Paschen, W. Carrillo-Cabrera, A. Bentien, V. H. Tran, M. Baenitz, Yu. Grin, and F. Steglich, Phys. Rev. B **64**, 214401 (2002).
[19] G. S. Nolas and C. A. Kendziora, Phys. Rev. B **62**, 7157 (2000).
[20] V. Keppens, B. C. Sales, D. Mandrus, B. C. Chakoumakos, and C. Laermans, Philos. Mag. Lett. **80**, 807 (2000).
[21] V. Keppens, M. A. McGuire, A. Teklu, C. Laermans, B. C. Sales, D. Mandrus, and B. C. Chakoumakos, Physica B **316-317**, 95 (2002).
[22] J. Dong, O. F. Sankey, G. K. Ramachandran, and P. F. McMillan, J. Appl. Phys. **87**, 7726 (2000).
[23] J. Dong, O. F. Sankey, and C. W. Myles, Phys. Rev. Lett. **86**, 2361 (2001).
[24] M. Menon, E. Richter, and K. R. Subbaswamy, Phys. Rev. B **56**, 12290 (1997).
[25] D. Kahn and J. P. Lu, Phys. Rev. B **56**, 13898 (1997).
[26] J. Dong, O. F. Sankey, and G. Kern, Phys. Rev. B **60**, 950 (1999).
[27] J. Dong and O. F. Sankey, J. Phys.: Condens. Matter **11**, 6129 (1999).
[28] Y. Guyot, B. Champagnon, E. Reny, C. Cros, M. Pouchard, P. Melinon, A. Perez, and J. Gregora, Phys. Rev. B **57**, R9475 (1998).
[29] S. Bobev and S. C. Sevov, J. Am. Chem. Soc. **121**, 3795 (1999).

[30] S. Bobev and S. C. Sevov, J. Solid State Chem. **153**, 92 (2000).
[31] G. S. Nolas, D. G. Vanderveer, A. Wilkinson, and J. L. Cohn, J. Appl. Phys. **91**, 8970 (2002).
[32] G. K. Ramachandran, J. Dong, O. F. Sankey, and P. McMillan, Phys. Rev. B **63**, 33102 (2000).
[33] S. Latturner, B. B. Iverson, J. Sepa, V. Srdanov, and G. Stucky, Phys. Rev. B **63**, 125403 (2001).
[34] VASP is the ''Ab-initio Simulation Program,'' developed at the Institute für Theoretische Physik of the Technische Universitaät Wien; G. Kresse and J. Furthmüller, Comput. Mater. Sci. **6**, 15 (1996).
[35] G. Kresse and J. Hafner, Phys. Rev. B **47**, 558 (1993).
[36] G. Kresse and J. J. Furthmüller, Phys. Rev. B **55**, 11169 (1996).
[37] See, for example, O. Madelung, *Semiconductors Basic Data*, 2nd ed. (Springer-Verlag, Berlin, 1996), and references therein.